ROLE OF TOPOGRAPHY AND ANISOTROPY WHEN SELECTING UNLINED PRESSURE-TUNNEL ALIGNMENT

By Bernard Amadei,[1] and Ernian Pan,[2] Associate Members, ASCE

ABSTRACT: This paper shows how analytical solutions, proposed by the writers to predict in-situ stresses in rock masses with smooth and irregular topographies, can help in the selection of the alignment of unlined pressure tunnels near slopes and valley walls. The proposed methodology can be applied to ridges and valleys in isotropic or anisotropic rock masses subject to gravity or to combined gravitational and tectonic loading. The analytical solutions are two-dimensional and assume plane or generalized plane strain. They can be used to substitute existing design charts for pressure tunnels based on the finite-element method. It is found that the safe alignment of unlined pressure tunnels depend greatly on the extent of tensile regions in valley walls, which itself depends on parameters such as valley geometry, the degree of rock anisotropy, the orientation of the planes of rock anisotropy, and the in-situ loading conditions (gravity, gravity and tectonic).

INTRODUCTION

Pressure tunnels, which are unlined over most of their lengths have been used in various hydroelectric schemes around the world and have been called on to perform under increasingly higher heads, now approaching 1,000 m (Benson, unpublished paper, 1988). The first and foremost consideration in the safe design of unlined pressure tunnels is that water leakage by hydraulic opening (hydraulic jacking) of the rock mass be avoided. Water leakage may lead to disastrous and expensive consequences as illustrated in many case studies (Broch 1984; Sharma et al. 1991; Brekke and Ripley 1993). Hydraulic jacking can be prevented by positioning unlined pressure tunnels in competent rock and under enough rock cover to provide confinement and watertight conditions. Another alternative is to use steel liners, which tend to be costly.

Several criteria have been proposed in the literature to determine the safe position of pressure tunnels near slopes or valley walls (Broch 1984a; Brekke and Ripley 1993). One empirical criterion, used successfully in many hydroelectric projects, was first proposed by Bergh-Christensen and Dannevig in 1971 (Broch 1984). The criterion is that at each point along the pressure-tunnel alignment the minimum rock cover, L, taken as the shortest distance to the valley slope surface and shown in Fig. 1, must be equal to

$$L = \frac{\gamma_w h_w F}{\gamma \cos \beta} \tag{1}$$

where h_w = static water head at the point of the tunnel under consideration; β = average slope angle of the valley side (less than 60°); γ_w and γ = unit weights of the water and the rock mass, respectively; and F = a safety factor. For a near-horizontal topography ($\cos \beta \approx 1$), (1) reduces to the traditional criterion where the minimum rock cover must be equal to $\gamma_w h_w F/\gamma$; that is, the vertical stress associated with the overburden rock must always exceed the water pressure at any point along the tunnel.

Another criterion proposed by Selmer-Olsen (1974) is based on the concept of using numerical methods, such as the finite-element method, to determine the state of in-situ stress in valley sides. The location of a pressure tunnel is selected based on the condition that nowhere along its alignment should the internal water pressure exceed the minimum in-situ principal stress, σ_3, in the surrounding rock mass (compression being positive). Mathematically, this criterion can be expressed as follows:

$$\sigma_3 > \gamma_w h_w \tag{2}$$

Design charts based on the finite-element method have been proposed for idealized valley geometries and topographies and for idealized rock mass properties.

Using the finite-element method to determine the in-situ state of stress for selecting the alignment of pressure tunnels has several limitations. First, the method is restricted to finite domains. Second, the results tend to be mesh-dependent and errors can arise when selecting the boundary conditions of the domain of interest. Third, most pressure-tunnel design charts obtained with the finite-element method are based on the assumption that the rock mass is continuous, homogeneous, and isotropic. The effect of rock mass fabric such as bedding, foliation, or jointing on in-situ stress distribution and magnitude is usually not taken into account. Fourth, the model topography is very much simplified and idealized. Fifth, most finite-element analyses are two-dimensional and assume plane-strain conditions. Finally, the stress perpendicular to the model plane is assumed to be the intermediate principal stress (Broch 1984a), which is not always mechanically correct even under plane strain.

As the aim in pressure-tunnel design is to maximize the tunnel length, which stays unlined with a minimum risk of water leakage, knowledge of the in-situ stress field along the proposed tunnel alignment is critical. Stress measurements using techniques such as overcoring, hydraulic fracturing, or hydraulic jacking tests (Price Jones and Sims 1984; Enever et al. 1992) are required to finalize the design of pressure tunnels. For preliminary design, however, estimating in-situ

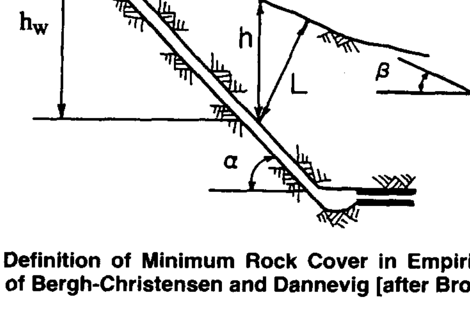

FIG. 1. Definition of Minimum Rock Cover in Empirical Design Criterion of Bergh-Christensen and Dannevig [after Broch (1984a)]

[1]Prof., Dept. of Civ. Engrg., Univ. of Colorado, Boulder, CO 80309-0428.

[2]Res. Assoc., Dept. of Civ. Engrg., Univ. of Colorado, Boulder, CO.

Note. Discussion open until May 1, 1996. To extend the closing date one month, a written request must be filed with the ASCE Manager of Journals. The manuscript for this paper was submitted for review and possible publication on December 5, 1994. This paper is part of the *Journal of Geotechnical Engineering*, Vol. 121, No. 12, December, 1995. ©ASCE, ISSN 0733-9410/95/0012-0879-0885/$2.00 + $.25 per page. Paper No. 9737.

stresses may be sufficient. Estimation of in-situ stresses can also be useful when selecting the most appropriate in-situ stress measuring techniques and the location of the stress measurements.

The exact prediction of in-situ stresses in rock and their variation is, for all practical purposes, impossible. Estimating in-situ stresses is a difficult process and requires a detailed characterization of the rock and considerable judgment. Models (physical or numerical) can be developed to explore the importance of such parameters as the rock's constitutive model, its loading history, geologic structures, and the boundary conditions on in-situ stresses. Numerical estimation of in-situ stresses can be carried out using the finite-element method or other numerical methods available in rock mechanics (boundary-element and discrete-element methods).

This paper aims to show how analytical solutions, proposed by the writers (Pan and Amadei 1994; Pan and Amadei, in press, 1995) to predict in-situ stresses in isotropic or anisotropic rock masses with smooth and irregular topographies, can help in the selection of the alignment of unlined pressure tunnels near slopes and valley walls. The rock masses can be subjected to gravity or to combined gravitational and tectonic loading. The analytical solutions are two-dimensional and assume plane or generalized plane strain. The solutions can be used to substitute existing design charts for pressure tunnels, based on the finite-element method. The effect of rock anisotropy, gravity, tectonic stresses, and geometry of the topography on in-situ stresses can be taken into account. At the outset, this paper presents a review of the different analytical methods available to estimate the effect of topography on in-situ stresses. The way the analytical solutions developed by the writers can be incorporated into a no-leakage criterion to pressure-tunnel alignment is also shown. Finally, examples are presented to illustrate the effect of valley geometry, the degree of rock anisotropy, the orientation of the planes of rock anisotropy, and in-situ loading conditions (gravity, gravity and tectonic) on the selection of pressure-tunnel alignment near valley walls.

EFFECT OF TOPOGRAPHY ON IN-SITU STRESSES

When estimating the state of stress at any point in a rock mass, several assumptions are usually made. First, the state of stress is described by two components: a vertical component due to the weight of overlying rock at that depth, and a horizontal component equal to several times or a fraction of the vertical stress. Second, the horizontal stress is assumed to be uniform in the horizontal plane. Finally, the vertical and horizontal stresses are assumed to be principal stresses. In general, these simplifying assumptions break down when the ground surface is not horizontal. At the ground surface, principal stresses are parallel and perpendicular to the topography in the absence of surface loads. With depth, the principal stresses turn and approach the same directions as when the ground surface is horizontal. Stress measurements showing the effect of topography have been reported by several authors [Judd (1964), Chaplow and Eldred (1984), Haimson (1984), Myrvang (1993), among others].

The effect of surface topography on in-situ stresses has been modeled in the literature using different analytical methods. One is the exact conformal mapping method as studied by Akhpatelov and Ter-Martirosyan (1971), Ter-Martirosyan et al. (1974), Ter-Martirosyan and Akhpatelov (1972), Savage et al. (1985), and Savage (1994) for gravity loading only, and by Savage and Swolfs (1986) for gravity and tectonic loading. However, this approach is restricted to isotropic media, to the very few smooth topographic profiles for which conformal mapping functions can be found exactly, and to two-dimensional problems. Another approach for two- and three-dimensional problems in isotropic media is the perturbation method discussed by McTigue and Mei (1981, 1987), McTigue and Stein (1984), and Liu and Zoback (1992). Liao et al. (1992) also used the perturbation method for two-dimensional problems in anisotropic rock masses. The advantage of the perturbation method is that it can handle any smooth topographic feature. However, the solutions derived with that method are restricted to topographies with small slopes not exceeding 10%.

In spite of their limitations, all the solutions derived with the exact conformal mapping and perturbation methods clearly show that the topography can have a major effect on the magnitude and distribution of in-situ stresses. For instance, the expressions in Savage et al. (1985) for gravitational stresses in long symmetric isotropic ridges and valleys clearly depend on the geometry of the topography and on the rock's Poisson's ratio. It was found that: (1) Nonzero horizontal compressive stresses develop at and near ridge crests; and (2) horizontal tensile stresses develop under valleys. The horizontal compressive stresses in ridge crests decrease and the horizontal tensile stresses in valleys become more compressive with an increasing Poisson's ratio. As shown by Savage and Swolfs (1986), superposing the effect of a uniaxial tectonic compression acting normal to the axial planes of isolated symmetric ridges and valleys on the gravitational stresses results in a slight increase in the lateral component of compressive stresses at the ridge crests. Under the valley bottoms, this superposition results in a decrease in the tensile stresses. The opposite effects occur when a far-field tectonic tension is superposed on the gravitational stress field. McTigue and Mei (1981, 1987) and Liao et al. (1992) also showed that topography affects gravitational stress distributions even in areas of low regional slopes.

Because of the limitations of the conformal mapping and perturbation methods, numerical methods were, until recently, the only other alternative to determine in-situ stresses in rock masses with complex topographies. However, the limitations can be overcome with a new analytical method proposed by Pan and Amadei (1994) to determine the stress field in a homogeneous, general anisotropic, and elastic half-space subject to gravity and surface loads under a condition of generalized plane strain and limited by irregular (but smooth) outer boundaries. More recently, the method was extended to account for the effect of uniform far-field stresses associated with tectonic loading (Pan and Amadei, in press, 1995). In the analytical solutions, the stresses are expressed in terms of three analytical functions that can be determined using a numerical conformal mapping method and an integral equation method. The solutions were used to determine the stresses induced by gravity in long symmetic and asymmetric ridges and valleys (Pan and Amadei 1993; Pan et al. 1994), as were the stresses induced by gravity or combined gravity and uniaxial horizontal tectonic loading in symmetric and asymmetric ridges and valleys (Pan et al. 1995). Parametric studies were conducted for transversely isotropic ridges and valleys with planes of anisotropy striking parallel to the ridge or valley axis. The effect of topography, orientation of anisotropy, and degree of anisotropy on the magnitude and distribution of gravitational stresses was investigated.

The parametric studies conducted by Savage et al. (1985), Savage and Swolfs (1986), Liao et al. (1992), Pan and Amadei (1993), Pan et al. (1994), and Pan et al. (1995) show the existence of a zone of tensile stresses developing at and near valley bottoms in isotropic rock and transversely isotropic rock, with planes of transverse isotropic parallel to the valley axis. The existence of such a zone is critical: (1) When selecting the alignment of pressure tunnels near slopes and valley walls; and (2) in deciding where unlined tunnel sections end and steel lining starts. More specifically, the parametric studies show the following trends:

1. For symmetric valleys under gravity only, the maximum tensile stress is at the valley bottom and the zone of tension is symmetric for isotropic rock and for transversely isotropic rock with vertical and horizontal planes of anisotropy. If the planes of anisotropy are inclined, the tensile region is no longer symmetric and extends on the side of the valley that is dipping in the same direction as the planes of anisotropy. The other side of the valley experiences more of a compressive state of stress.
2. For symmetric valleys under gravity only, and for a given dip angle of the planes of rock anisotropy, the extent of the tensile region depends on the rock elastic properties. In particular, the size of the tensile region decreases as the ratio between the rock modulus parallel to the planes of anisotropy and that normal to the planes of anisotropy increases (or in other words as the rock becomes more deformable in the direction normal to the planes of anisotropy). For both isotropic and anisotropic rocks, the tensile stresses become more compressive with increasing Poisson's ratio(s).
3. For symmetric valleys under gravity only, the tensile region decreases as the valleys become narrower.
4. For asymmetric valleys under gravity only, trends similar to those for symmetric valleys can be found. However, the tensile zone at the valley bottom is no longer symmetric and its shape depends on the topography.
5. For symmetric and asymmetric valleys, addition to the gravity of a horizontal uniaxial compressive tectonic stress normal to the valley axis diminishes the tension in valley bottoms.

There is field evidence to support the existence of tensile stresses near valley bottoms. For instance, Knill (1968) found that there is usually a zone near the valley surface in which the rock mass is loose and discontinuous. Because of this, Knill suggested that underground excavation, tunnelling, or dam foundation be carried well below this zone. Another evidence for valley-bottom tensile stress is rebound near valley bottoms and valley walls, as noted by Matheson and Thomson (1973). This upwarping phenomenon may be considered a result of tensile stresses (Matheson and Thomson 1973; Silverstri and Tabib 1983). James (1991) also described the evidence of tensile stresses near valley bottoms, such as bed separation and bedding fractures at the toes of deep valleys and open (tension) joints deep into valley sides. By conducting a survey on the nature and frequency of coal-mine roof failure beneath valleys, Molinda et al. (1992) found that 52% of the unstable roof cases in the surveyed mines occurred directly beneath the bottommost part of the valley. The survey also showed that broad, flat-bottomed valleys were more likely to be sites of hazardous roof conditions than narrow-bottomed valleys. They also found evidence of valley stress relief beneath several valleys in the form of bedding plane faults and low-angle thrust faults at mining depths as great as 100 m.

NO-LEAKAGE CONDITION

Consider the equilibrium of an anisotropic half-space with the geometry of Fig. 2. The half-space represents a rock mass with an irregular topography. The medium in the half-space is assumed to be linearly elastic, homogeneous, transversely isotropic, and continuous with a uniform density ρ. An x-, y-, and z-coordinate system is attached to the half-space so that the x- and z-axes are in the horizontal plane and the y-

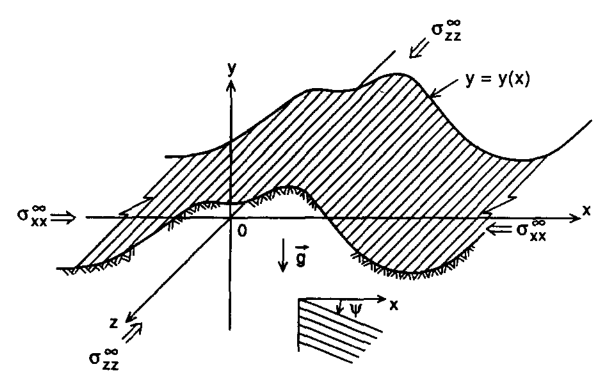

FIG. 2. Geometry of Problem: Anisotropic Half-Space with Irregular Topography

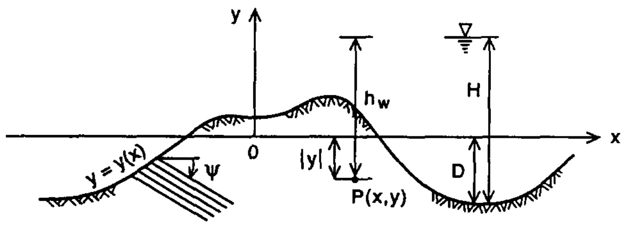

FIG. 3. Definition of Variables for No-Leakage Condition

axis points upward. The half-space is subject to gravity, $\vec{g}$, acting in the $-y$ direction, and to far-field horizontal and uniform tectonic stresses, σ_{xx}^{∞} and σ_{zz}^{∞}, acting in the x- and z-directions, respectively. The half-space geometry and the rock mass elastic properties are assumed to be independent of the z-direction. The boundary curve of the half-space is defined by an analytic function $y = y(x)$ as follows:

$$y(x) = \sum_{i=1}^{N} y_i(x) \tag{3}$$

with

$$y_i(x) = \frac{a_i^2 b_i}{(x - x_i)^2 + a_i^2} \tag{4}$$

Eqs. (3) and (4) correspond to the geometric superposition of $i = 1, N$ symmetric ridges or valleys $y = y_i(x)$ centered at $x = x_i$. If b_i is positive, (4) corresponds to a ridge of height b_i. If b_i is negative, (4) corresponds to a valley with depth $|b_i|$. The parameter a_i controls the lateral extent of each ridge or valley with inflection points located at $x = x_i \pm a_i/\sqrt{3}$, $y = 0.75b_i$, at which the slopes are equal to $\pm 3b_i\sqrt{3}/(8a_i)$ (Pan et al. 1994). Thus, different, complex, and smooth topographies can be obtained by choosing different, positive, or negative values of a_i, b_i, and x_i for $i = 1, N$.

The planes of transverse isotropy in the rock mass are assumed to strike parallel to the z-axis and to dip at an angle ψ in the $+x$-direction. In a coordinate system attached to the planes of transverse isotropy, the rock mass deformability is described by five elastic properties: E, E', ν, ν', and G' where: (1) E and E' are Young's moduli in the plane of transverse isotropy and in the direction normal to it, respectively; ν and ν' are Poisson's ratios characterizing the lateral strain response in the plane of transverse isotropy to a stress acting parallel and normal to it, respectively; and (3) G' is the shear modulus in planes normal to the plane of transverse isotropy.

Consider the geometry of Fig. 3, which shows an xy cross section of the half-space in Fig. 2. The first step in the proposed methodology is to analytically determine the magnitude and distribution of the in-situ stresses induced by gravitational and/or tectonic loading of the half-space. This can be done

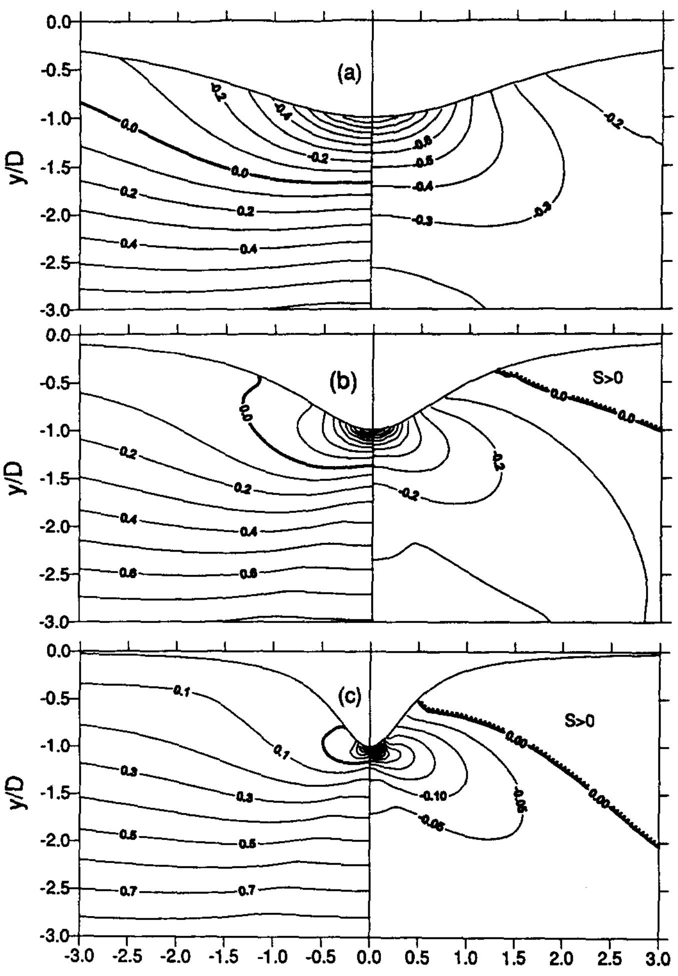

FIG. 4. Contours of $\sigma_3/\gamma D$ and S for Three Symmetric Valleys Where $b/D = -1$ and a/D is: (a) 2.0; (b) 1.0; (c) 0.5

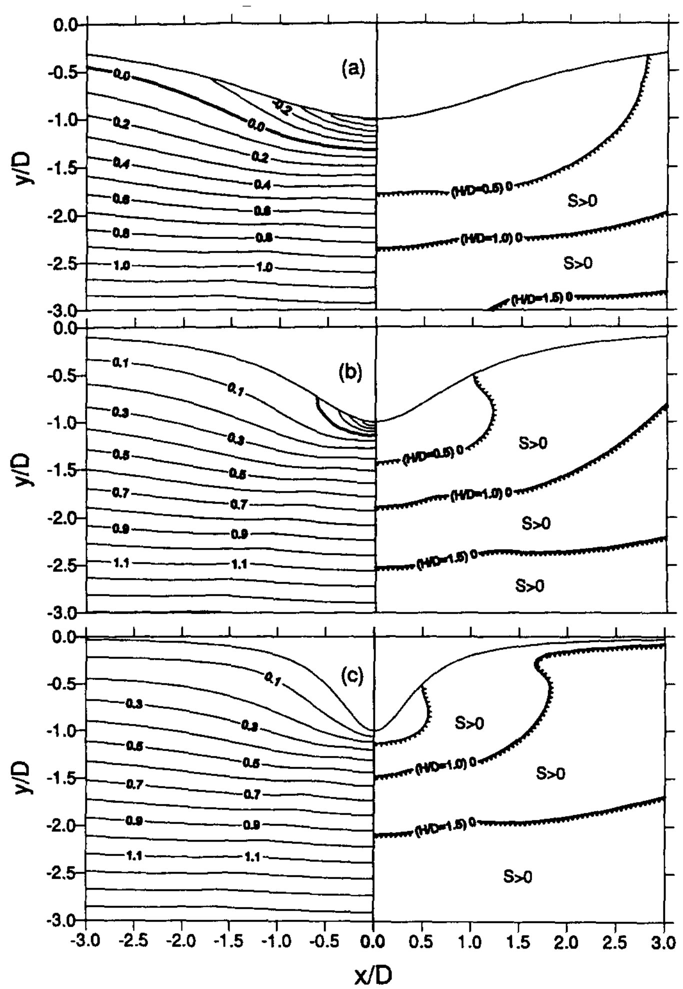

FIG. 5. Contours of $\sigma_3/\gamma D$ and $S = 0$ for Three Symmetric Valleys Where $b/D = -1$ and a/D is: (a) 2.0; (b) 1.0; (c) 0.5

using the analytical solution suggested by Pan and Amadei (1994) and Pan and Amadei (in press, 1995). It is shown that for the orientation of the planes of transverse isotropy and the tectonic stresses considered here, the rock mass deforms in plane strain in the xy-plane. In addition, at each point $P(x,y)$, two of the three principal stresses are local in the x, y-plane and the longitudinal stress in the z-direction is the third principal stress. The smallest of the three principal stresses is defined as σ_3.

The second step is to compare σ_3 with the water pressure at $P(x,y)$, equal to $\gamma_w h_w$. At that point, the static water head h_w, is equal to $H - y - D$, where H is the maximum static water head and D is a characteristic depth of the topography. Thus, the no-leakage criterion defined in (2) can be rewritten in dimensionless form as follows:

$$S = \frac{\sigma_3}{\gamma D} - \frac{\gamma_w}{\gamma}\left[\frac{H}{D} - \frac{y}{D} - 1\right] > 0 \tag{5}$$

Contour diagrams of S can be generated for different types of topography, rock mass properties, rock mass loading conditions (gravity, gravity and tectonic), and different values of the ratio H/D. The contour $S = 0$ corresponds to the balance between the increasing water pressure and the increasing minor in-situ principal stress. The domain $S > 0$ corresponds to the region in the rock mass in which unlined pressure tunnels can be placed without leakage. If a safety factor against leakage F is introduced, the critical contour is no longer $S = 0$, but $S = S_c$ with

$$S_c = \frac{\sigma_3}{\gamma D} - F\frac{\gamma_w}{\gamma}\left[\frac{H}{D} - \frac{y}{D} - 1\right] \tag{6}$$

In general, S and S_c depend on the following parameters: (1) Four ratios of elastic constants E/E', G/G', ν, ν', and the dip angle ψ of the planes of transverse isotropy; (2) the rock's relative density γ/γ_w; (3) the ratio between the maximum static water head H and a characteristic depth D of the topography; (4) the coordinates x/D and y/D of the point $P(x,y)$ at which the leakage criterion is verified; (5) the ratios a_i/D, b_i/D, and x_i/D for $i = 1, N$ defining the geometry of the topography; (6) the ratios $\sigma_{xx}^{\infty}/\gamma D$ and $\sigma_{zz}^{\infty}/\gamma D$ when tectonic loading is active in the x,z horizontal plane; and (6) the value of the safety factor F.

NUMERICAL EXAMPLES

An initial illustrative example, Figs. 4(a–c) show contours of the minimum principal stress $\sigma_3/\gamma D$ (left-hand side) and contours of S (right-hand side) for three symmetric valleys with $b/D = -1$ and $a/D = 2$, 1, and 0.5, respectively. The ratio H/D is equal to 0.5. The rock is assumed to be isotropic with a Poisson's ratio of 0.25 ($E/E' = G/G' = 1$, $\nu = \nu' = 0.25$). Figs. 4(a–c) indicate that as a/D decreases, or in other words as the valley walls become steeper, the zone where $\sigma_3/\gamma D$ is tensile (negative) decreases in size and the no-leakage region ($S > 0$) becomes larger. For higher values of the maximum static head H, with H/D equal to 1.0 and 1.5, it can be shown that S is always negative over the domain considered here.

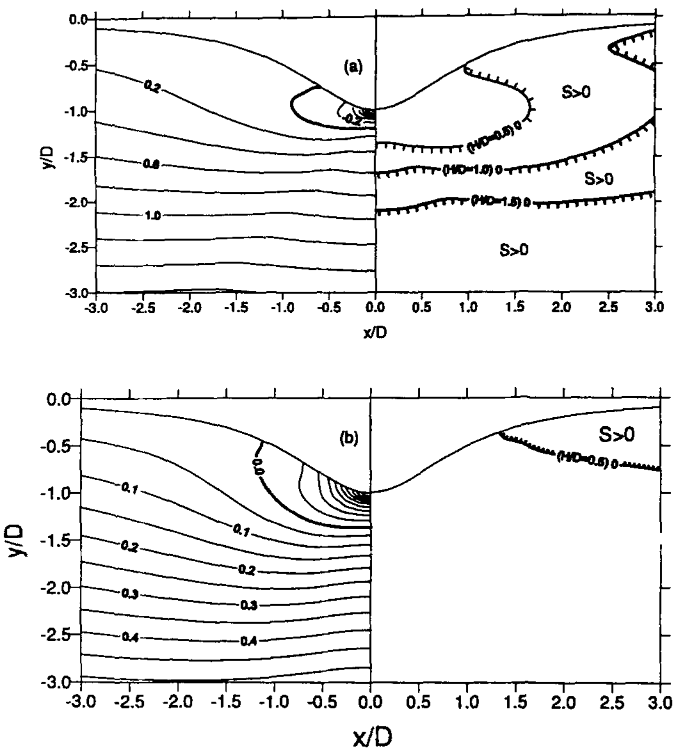

FIG. 6. Contours of $\sigma_3/\gamma D$ and S = 0 for Symmetric Valley With b/D = −1 and a/D = 1.0, Where Planes of Rock Anisotropy are: (a) Horizontal; (b) Vertical

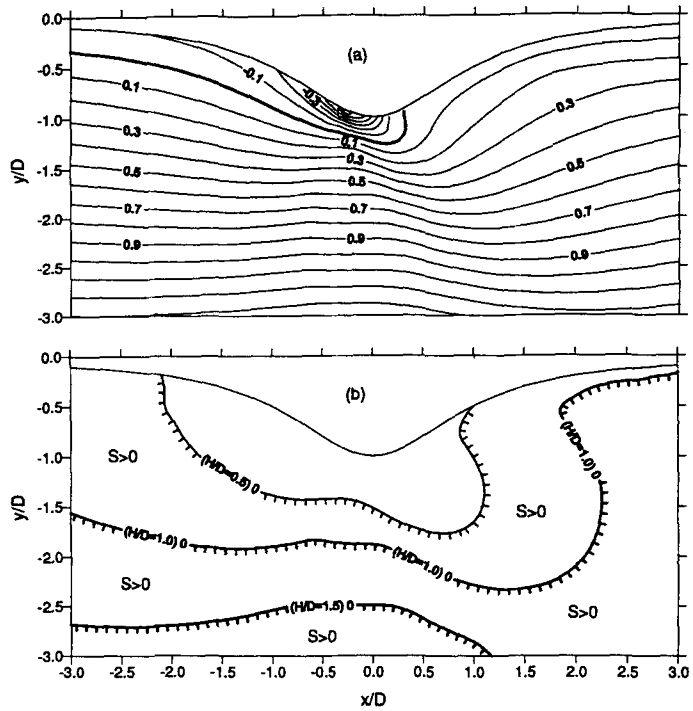

FIG. 7. Contours for Symmetric Valley with b/D = −1 and a/D = 1.0, Where Planes of Rock Anisotropy Dip at 45° to the Right: (a) $\sigma_3/\gamma D$; (b) S = 0

Figs. 5(a–c) show contours of $\sigma_3/\gamma D$ (left-hand side) for the same three valley geometries considered in Figs. 4(a–c), except that the rock's Poisson's ratio is now equal to 0.35 instead of 0.25. The right-hand sides of Figs. 5(a–c) show three $S = 0$ contours for H/D = 0.5, 1.0, and 1.5. Again, as the valley walls become steeper, the zone where $\sigma_3/\gamma D$ is tensile (negative) decreases in size (and even vanishes for a/D = 0.5) and the no-leakage region ($S > 0$) becomes larger for a given value of H/D. As expected, for a given valley geometry, the extent of the no-leakage region ($S > 0$) increases as the maximum static water head, H, decreases. Comparison between Fig. 5 and Fig. 4 indicates that, for a given valley geometry, an increase in the rock's Poisson's ratio: (1) Reduces the extent of the tensile zone at and near valley bottoms; and (2) increases the extent of the no-leakage region ($S > 0$) for a given value of the H/D ratio.

The effect of rock anisotropy on the distribution of $\sigma_3/\gamma D$ and the extent of the no-leakage region ($S > 0$) for H/D = 0.5, 1.0, and 1.5 is demonstrated in Figs. 6–9. The rock is

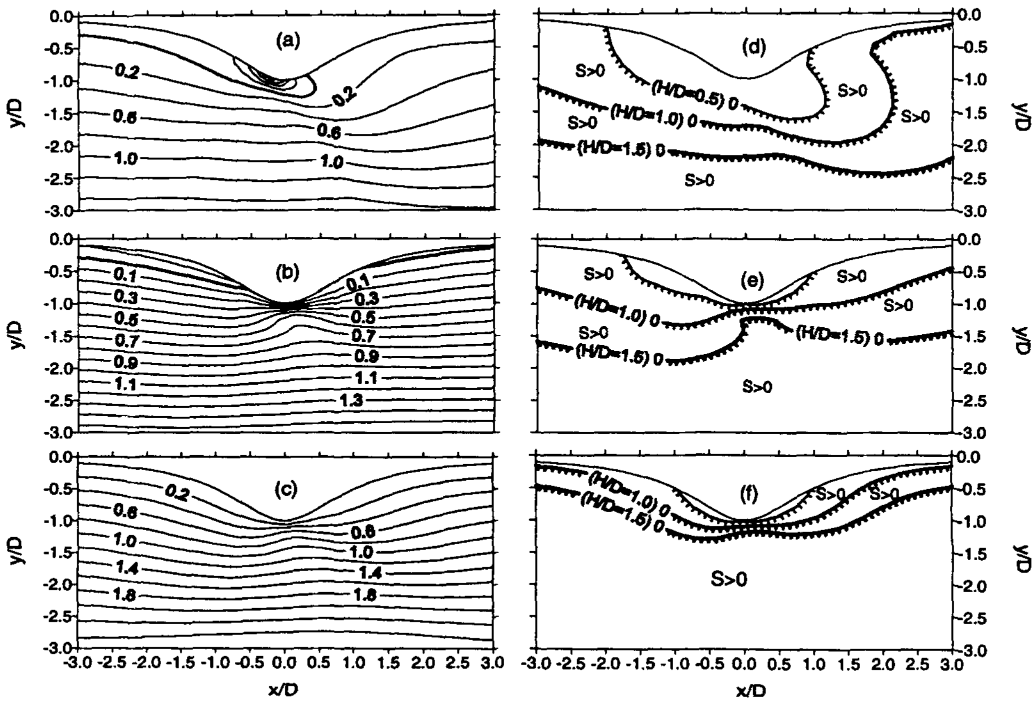

FIG. 8. Contours for Symmetric Valley with b/D = −1 and a/D = 1.0, Where Planes of Rock Anisotropy Dip at 30° to the Right: (a–c) $\sigma_3/\gamma D$, (d–f) S = 0

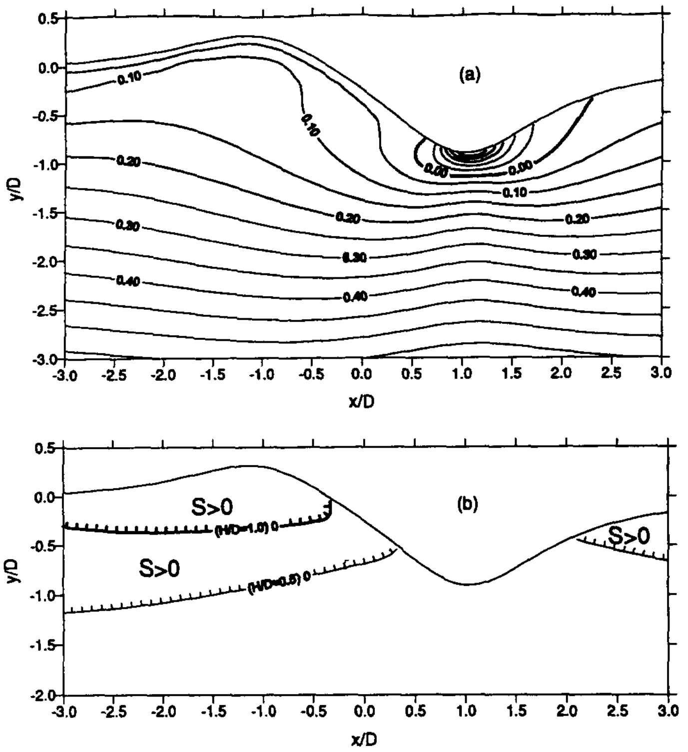

FIG. 9. Contours for Nonsymmetric Valley formed by Superposition of Two Symmetric Valleys, Where Rock Mass has Vertical Planes of Rock Anisotropy: (a) $\sigma_3/\gamma D$; (b) $S = 0$

now strongly transversely isotropic with $E/E' = G/G' = 3$, $\nu = 0.25$, and $\nu' = 0.15$.

Figs. 6(a), 6(b), and 7(a), 7(b) show the contours for $\sigma_3/\gamma D$ and $S = 0$ when the planes of rock anisotropy are horizontal, vertical, and dipping at $\psi = 45°$ in the $+x$-direction. In both Figs. 6 and 7 the contours of $S = 0$ are obtained for $H/D = 0.5$, 1.0, and 1.5. The valley is symmetric with the same geometry as in Figs. 4(b) and 5(b), with $b/D = -1$ and $a/D = 1$. Comparison of Fig. 6(a), 6(b), and 7(a), 7(b) with Fig. 4(b) reveals several trends. First, horizontal planes of anisotropy give a smaller tensile region, larger values of $\sigma_3/\gamma D$ at a given depth, and larger no-leakage regions than the isotropic case. Second, when the planes of anisotropy are vertical the extent of the tensile zone and the no-leakage region is not much affected by the anisotropic nature of the rock. However, the effect of the valley on the distribution of $\sigma_3/\gamma D$ is felt at a much larger depth. Third, when the planes of anisotropy dip at an angle other than 0° or 90°, the tensile and no-leakage regions are no longer symmetric with respect to the axial plane of the valley. As shown in Figs. 7(a) and 7(b) for $\psi = 45°$, the tensile region is no longer symmetric and extends on the left-hand side of the valley which is dipping in the same direction as the planes of rock anisotropy. The right-hand side of the valley, on the other hand, experiences more of a compressive state of stress and is more favorable than the left-hand side with regard to positioning unlined pressure tunnels.

Figs. 8(a–c) show contours of $\sigma_3/\gamma D$ and Figs. 8(d–f) show three $S = 0$ contours for $H/D = 0.5$, 1.0, and 1.5. The valley geometry is the same as in Fig. 4(b), 6, and 7 except that the planes of rock anisotropy are now dipping at an angle of 30° in the $+x$-direction. The rock mass is: (1) Under gravity only in Figs. 8(a) and 8(d); (2) under gravity and in a uniaxial tectonic compressive stress field $\sigma_{xx}^{\infty}/\gamma D = 1$ in Figs. 8(b) and 8(e); and (3) under gravity and in a biaxial tectonic compressive stress field $\sigma_{xx}^{\infty}/\gamma D = \sigma_{zz}^{\infty}/\gamma D = 1$ in Figs. 8(c) and 8(f). Figs. 8(a–f) indicate that addition of far-field compressive stresses reduces the extent of the tensile region in the valley walls and bottom [the tensile region vanishes in Fig. 8(c)] and increases the extent of the no-leakage region on both sides of the valley.

Finally, Figs. 9(a) and 9(b) show contours of $\sigma_3/\gamma D$ and $S = 0$ for a nonsymmetric valley formed by the superposition of two symmetric valleys with $a_1/D = a_2/D = 1.0$, $b_1/D = 0.5$, $b_2/D = -1.0$, $x_1/D = -1$, and $x_2/D = 1.0$. The rock mass has vertical planes of rock anisotropy. Here, the tensile and no-leakage regions are not symmetric because of the asymmetry in the topography.

CONCLUSIONS

We have shown that the safe alignment of unlined pressure tunnels depends greatly on the extent of tensile regions in valley walls, which itself depends on parameters such as valley geometry, degree of rock anisotropy, orientation of the planes of rock anisotropy, and the in-situ loading conditions (gravity, gravity and tectonic). In this paper, the criterion used to determine the safe alignment of pressure tunnels is such that no leakage takes place if there is enough in-situ confinement. The no-leakage criterion used in this paper is, in essence, similar to that proposed by Selmer-Olsen (1974). The main difference is that in-situ stresses are now determined analytically instead of numerically. The effect of rock anisotropy, gravity, tectonic stresses, and geometry of the topography on in-situ stresses can be taken into account in a more rational and exact manner than was done earlier with the finite-element method.

Following Selmer-Olsen (1974), here hydraulic jacking is assumed to occur only along surfaces oriented perpendicular to the least in-situ stress component σ_3. This is a conservative assumption since, as pointed out by Brekke and Ripley (1993), the jacking pressure could be higher than σ_3 if jacking occurs along surfaces (joints, faults, foliation, etc.) that are inclined with respect to that stress component.

ACKNOWLEDGMENT

This research is funded in part by the National Science Foundation, Grant No. MS-9215397.

APPENDIX I. REFERENCES

Akhpatelov, D. M., and Ter-Martirosyan, Z. G. (1971). "The stressed state of ponderable semi-infinite domains." *Armenian Acad. Sci. Mech. Bull.*, 24(3), 33–40.

Brekke, T., and Ripley, B. D. (1993). "Design of pressure tunnels and shafts." *Comprehensive rock engineering*, J. A. Hudson, ed., Pergamon Press, Inc., Elmsford, N.Y., 349–369.

Broch, E. (1984a). "Development of unlined pressure shafts and tunnels in Norway." *Underground Space*, 8(3), 177–184.

Broch, E. (1984b). "Unlined high pressure tunnels in areas of complex topography." *Water Power and Dam Constr.*, 36(11), 21–23.

Chaplow, R., and Eldred, C. D. (1984). "Geotechnical investigations for the design of an extension to the Kariba South underground power station, Zimbabwe." *Proc., ISRM Symp. on Des. and Perf. of Underground Excavations*, E. T. Brown and J. A. Hudson, ed., British Geotech. Soc., London, England, 213–219.

Enever, J. R., Wold, M. B., and Walton, R. J. (1992). "Geotechnical investigations for the assessment of the risk of water leakage from pressure tunnels." *Proc., 6th Australia-New Zealand Conf. on Geomech.*

Haimson, B. C. (1984). "Pre-excavation in situ stress measurements in the design of large underground openings." *Proc., ISRM Symp. on Des. and Perf. of Underground Excavations*, E. T. Brown and J. A. Hudson, eds., British Getech. Soc., London, England. 183–190.

James, P. (1991). "Stress and strain during river downcutting." *Australian Geomech.*, 28–31.

Judd, W. R. (1964). "Rock stress, rock mechanics and research, in state of stress in the earth's crust. *Proc., Int. Conf. on State of Stress in Earth' Crust*, Elsevier, Appl. Sci., New York, N.Y. 5–54.

Knill, J. L. (1968). "Geotechnical significance of some glacially induced rock discontinuities." *Bull. Assoc. Engrg.*, Geology, Vol. 5, 49–62.
Liao, J. J., Savage, W. Z., and Amadei, B. (1992). "Gravitational stresses in anisotropic ridges and valleys with small slopes." *J. Geophys. Res.*, 97(B3), 3325–3336.
Liu, L., and Zoback, M. D. (1992). "The effect of topography on the state of stress in the crust: application to the site of the Cajon Pass Scientific Drilling Project." *J. Geophys. Res.*, 97(B4), 5095–5108.
McTigue, D. F., and Mei, C. C. (1981). "Gravity-induced stresses near topography of small slope." *J. Geophys. Res.*, 86(B10), 9268–9278.
McTigue, D. F., and Mei, C. C. (1987). "Gravity-induced stresses near axisymmetric topography of small slope." *Int. J. Numer. and Anal. Methods in Geomech.*, 11(3), 257–268.
McTigue, D. F., and Stein, R. S. (1984). "Topographic amplification of tectonic displacement: implications for geodetic measurement of strain changes." *J. Geophys. Res.*, Vol. 89, 1123–1131.
Matheson, D. S., and Thomson, S. (1973). "Geological implications of valley rebound." *Can. J. Earth Sci.*, Vol. 10, 961–978.
Molinda, M., Heasley, K. A., Oyler, D. C., and Jones, J. R. (1992). "Effects of horizontal stress related to stream valleys on the stability of coal mine openings." *BuMines RI 9413*, U.S. Bureau of Mines, U.S. Dept. of Interior, Washington, D.C.
Myrvang, A. M. (1993). "Rock stress and rock stress problems in Norway." *Comprehensive rock engineering*, J. A. Hudson, ed., Pergamon Press, Inc., Elmsford, N.Y., 461–471.
Pan, E., and Amadei, B. (1993). "Gravitational stresses in long asymmetric ridges and valleys in anisotropic rock." *Int. J. of Rock Mech. and Min. Sci., & Geomech. Abstr.*, 30(7), 1005–1008.
Pan, E., and Amadei, B. (1994). "Stresses in an anisotropic rock mass with irregular topography." *J. Engrg. Mech.*, ASCE, 120(1), 79–119.
Pan, E., Amadei, B., and Savage, W. Z. (1994). "Gravitational stresses in long symmetric ridges and valleys in anisotropic rock." *Int. J. of Rock Mech. and Min Sci. & Geomech. Abstr.*, 31(4), 293–312.
Pan, E., Amadei, B., and Savage, W. Z. (1995). "Gravitational and tectonic stresses in anisotropic rock with irregular topography." *Int. J. Rock Mech. and Min. Sci. & Geomech. Abstr.*, 32(3), 201–214.
Price Jones, A., and Sims, G. P. (1984). "Measurement of in-situ rock stresses for a hydro-electric scheme in Peru." *Proc., ISRM Symp. on Des. and Perf. of Underground Excavations*, E. T. Brown and J. A. Hudson, eds., British Geotech. Soc., London, England, 191–198.
Savage, W. Z. (1994). "Gravity induced stresses in finite slopes." *Int. J. of Rock Mech. and Min. Sci. & Geomech. Abstr.*, 31(5), 471–483.
Savage, W. Z., and Swolfs, H. S. (1986). "Tectonic and gravitational stress in long symmetric ridges and valleys." *J. Geophys. Res.*, 91(B3), 3677–3685.
Savage, W. Z., Swolfs, H. S., and Powers, P. S. (1985). "Gravitational stress in long symmetric ridges and valleys." *Int. J. of Rock Mech. and Min. Sci. & Geomech. Abstr.*, 22(5), 291–302.
Selmer-Olsen, R. (1974). "Underground openings filled with high pressure water or air." *Bull. Int. Assoc. Engrg. Geology*, Vol. 9, 91–95.
Sharma, V. M., Singh, R. B., Kuberan, R., Moza, K. K., and Sharma, T. (1991). "In-situ stress measurement for design of tunnels." *Proc., 7th Congr. Int. Soc. Rock Mech. (ISRM); Vol. 2*, A. A. Balkema, Rotterdam, The Netherlands, 1355–1358.
Silvestri, V., and Tabib, C. (1983a). "Exact determination of gravity stresses in finite elastic slopes. I: Theoretical considerations." *Can. Geotech. J.*, Ottawa, Canada, Vol. 20, 47–54.
Silvestri, V., and Tabib, C. (1983b). "Exact determination of gravity stresses in finite elastic slopes. Part II: Applications." *Can Geotech. J.*, Ottawa, Canada, Vol. 20, 55–60.
Ter-Martirosyan, Z. G., and Akhpatelov, D. M. (1972). "The stressed state of an infinite slope with a curvilinear boundary subject to a field of gravity and percolation." *J. Probl. Geomech.*, Vol. 5, 81–91.
Ter-Martirosyan, Z. G., Akhpatelov, D. M., and Manvelyan, R. G. (1974). "The stressed state of rock masses in a field body forces." *Proc., 3rd ISRM Congr., Part A*, 569–574.

APPENDIX II. NOTATION

The following symbols are used in this paper:

a_i, b_i = parameters describing topography;
D = characteristic depth of topography;
E, E' = Young's moduli;
F = safety factor against leakage;
G, G' = shear moduli;
H = maximum static water head;
h_w = static water head at a point in rock mass;
L = rock cover;
N = number of symmetric ridges or valleys;
x,y = coordinates of point $P(x,y)$;
x_i,y_i = coordinates;
β = average slope angle of valley side;
γ = unit weight of rock;
γ_w = unit weight of water;
ν, ν' = Poisson's ratios;
σ_3 = minimum in-situ principal stress; and
$\sigma_{xx}^\infty, \sigma_{zz}^\infty$ = far-field tectonic stresses in x-, and z-directions.